Atmospheric
Chemistry
and Physics

Supplement of

Influence of relative humidity on the heterogeneous oxidation of secondary organic aerosol

Ziyue Li et al.

Correspondence to: Ziyue Li (ziyli@ucdavis.edu) and Christopher D. Cappa (cdcappa@ucdavis.edu)

The supplemental material contains five figures that provide additional context or support for the material presented in the main text.
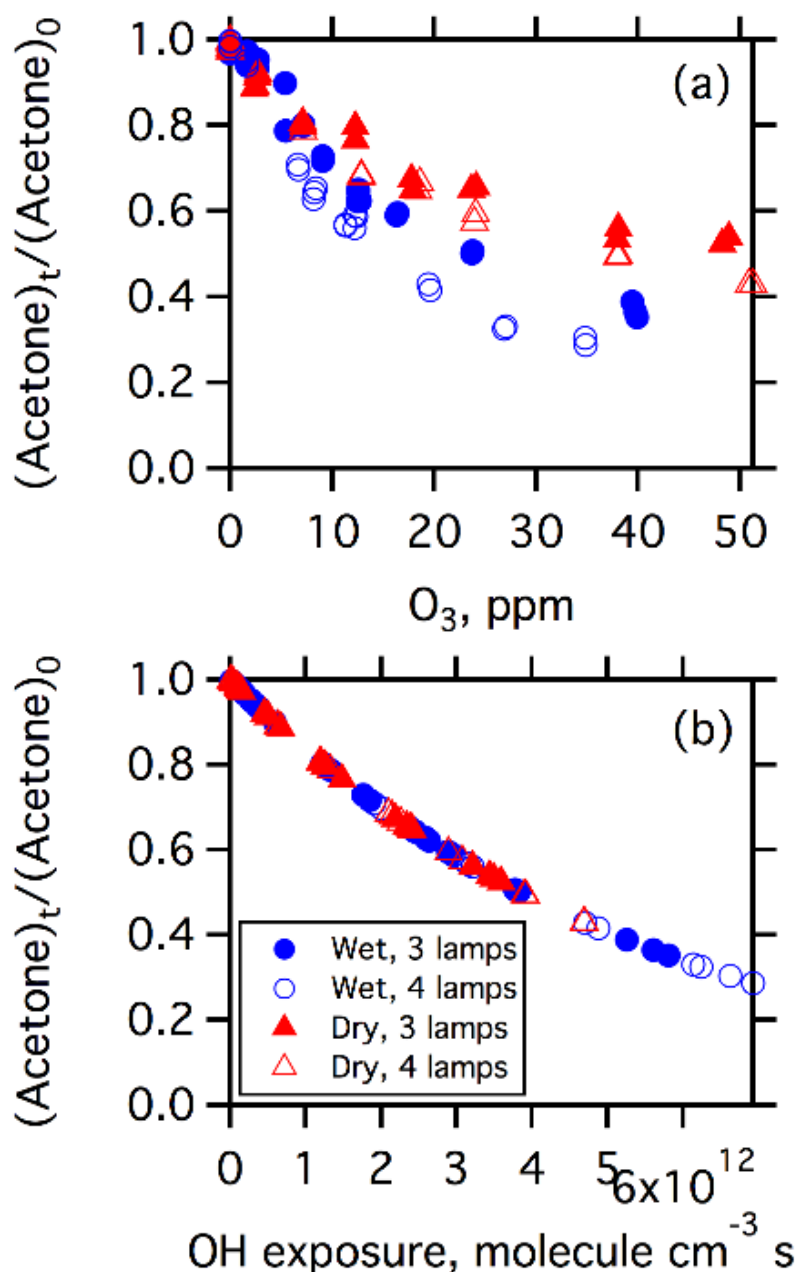
Figure S1. (a) The observed decay in the tracer compound (acetone) as a function of $[O_3]$, which is the precursor for OH radicals. **(b)** The relationship between the decay of acetone and the OH exposure calculated from Eqn. 1 in the main text. In both panels, results are shown for low RH (red triangles) and high RH (blue circles) conditions and solid and open markers denote experiments using different photon flux for radical production, with open markers indicating larger photon flux. In panel (a), a greater loss of acetone (i.e. smaller $(Acetone)_t/(Acetone)_0$) occurs for the same $[O_3]$ for high RH experiments compared to low RH experiments (red). For a given RH condition, greater loss of acetone is observed at a given $[O_3]$ for larger photon flux. These are in accordance with reactions R1 and R2 in the main text. In panel (b), the acetone decay/OH exposure relationship is independent of RH and photon flux.
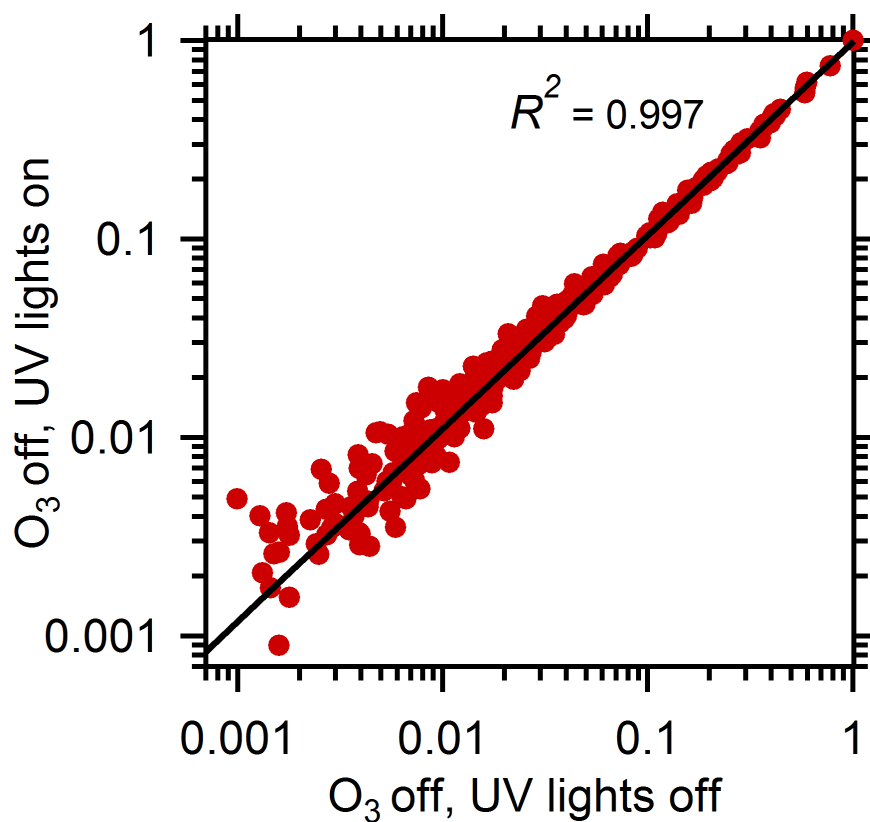
Figure S2. Scatter plot of the averaged mass spectrum of non-oxidized particles observed with no O_3 in the reaction flow tube and the UV lights on compared with the spectrum of non-oxidized particles observed with no O_3 in the reaction flow tube and the UV lights off. A linear fit yields R^2 = 0.997 and the slope from orthogonal distance regression is 0.974, which indicates no difference between two test conditions and a negligible impact of photolysis.
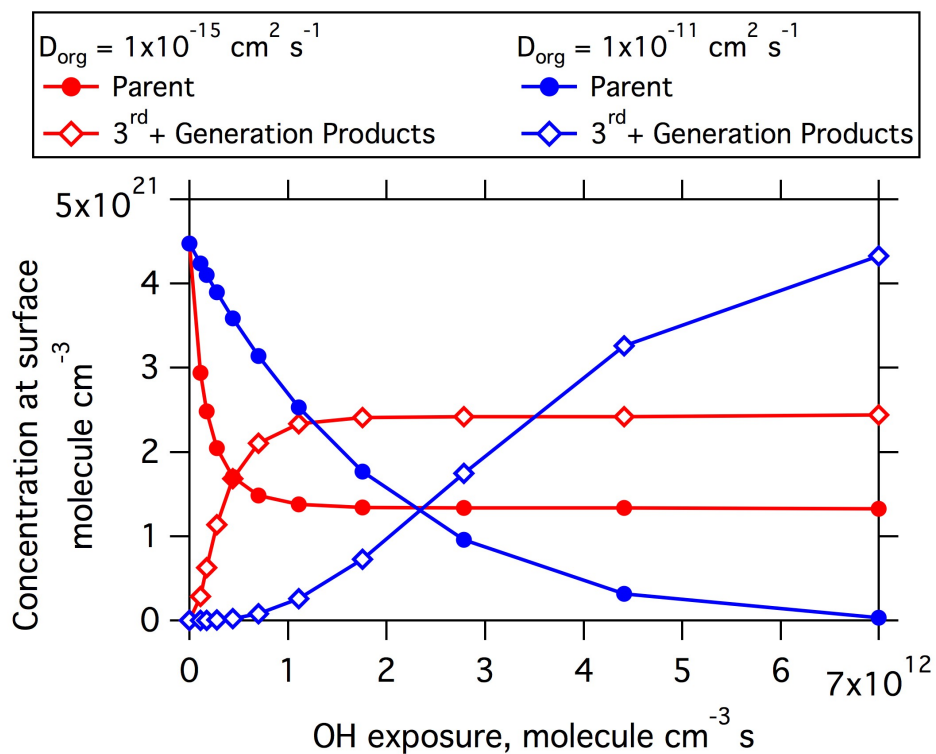
5

Figure S3. Variation in the concentration of the parent species (filled symbols) and 3rd and higher generation species (open symbols) in the surface layer for low-RH/small-D_{org} simulations (red lines/points) and for the high-RH/large-D_{org} simulations (blue lines/points). These are example results for simulations assuming γ = 0.5, p_{frag} = 0.31, GF = 1.0 and $k_{RO2+RO2}$ = 1×10^{-15} cm^3 molecule^{-1} s^{-1} (same conditions as Figure 10).
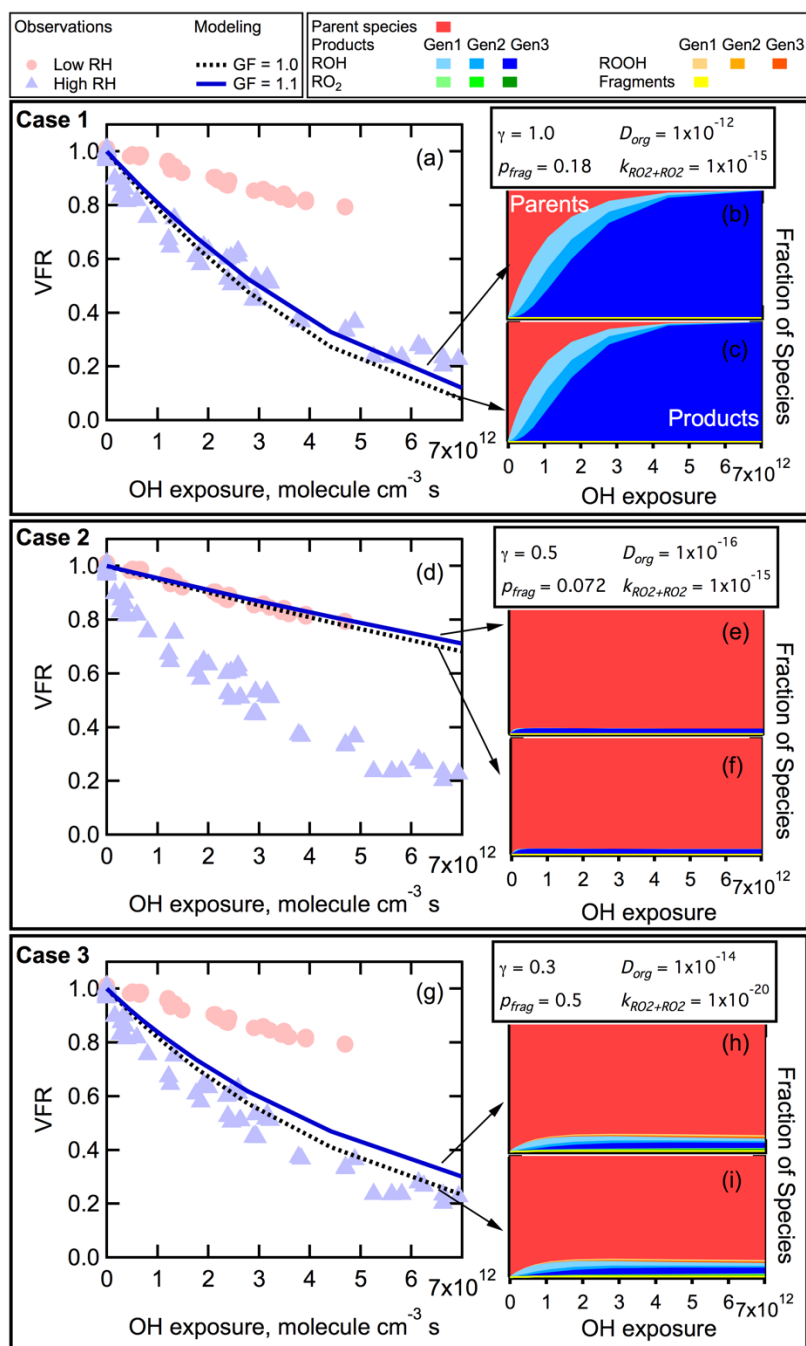
Figure S4. Comparison of simulation results using an RH-dependent *GF* with various combinations of RH-independent D_{org}, γ, p_{frag} and $k_{RO2+RO2}$. Three cases (unique combinations of D_{org}, γ, p_{frag} and $k_{RO2+RO2}$) are shown as examples. (Parameter values are in the figures. D_{org} has unit of cm^2 s^{-1} and $k_{RO2+RO2}$ has unit of cm^3 molecule^{-1} s^{-1}.) For each Case, three panels are shown. **(a, d, g)** Simulated volume loss with *GF* = 1.1 (blue solid line) or *GF* = 1.0 (black dashed line) compared to observation for high RH (blue triangles) and low RH (red circles). **(b, e, h)** Simulated compositional change with *GF* = 1.1. Parent species are shown as red and product species are shown as blue/orange/green shades. **(c, f, i)** Simulated compositional change with *GF* = 1.0. There is negligible difference between *GF* = 1 and *GF* = 1.1 for all cases indicating small impact of hygroscopic growth on composition evolution.
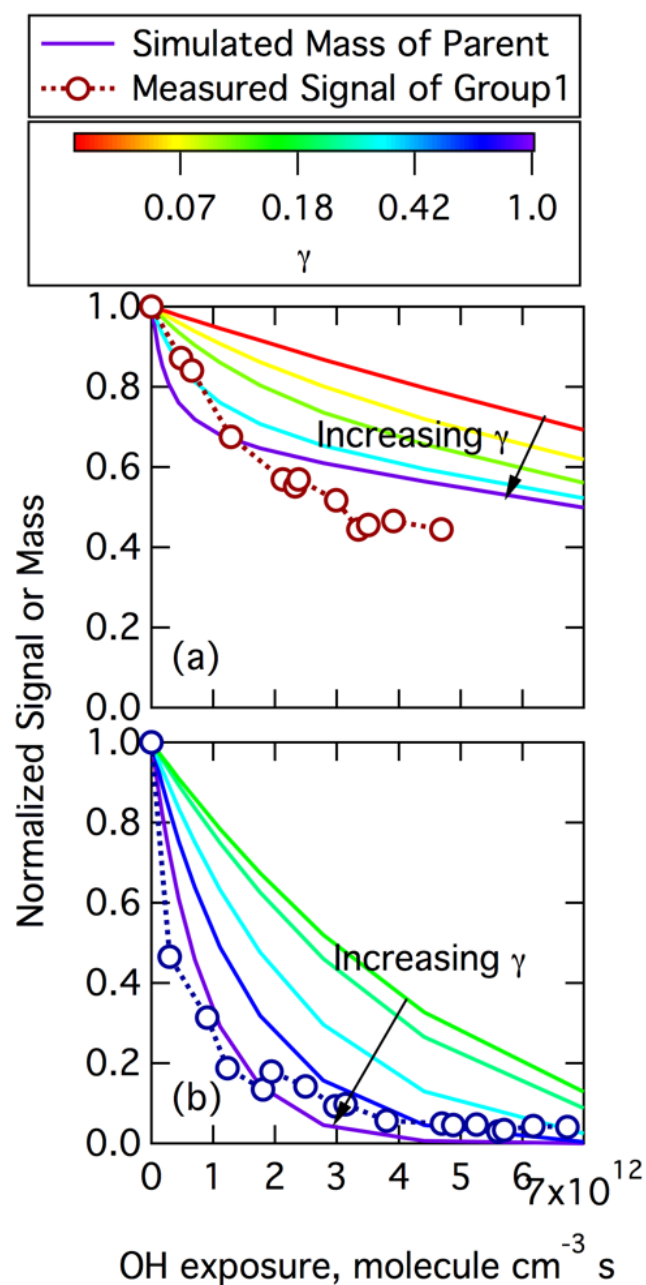
Figure S5. Simulated decay of the mass of parent species in the condensed phase as a function of OH exposure for varying γ (solid lines) compared to observed decay of the average signal of Group 1 ions signal (symbols and dashed lines) for low RH (a) and high RH (b). The γ used for simulations are denoted by colors with purple indicating $\gamma = 1.0$ (see legend; note log scale for γ). For each condition (low or high RH), p_{frag} are chosen in the simulations to produce best model-measurement agreement according to the γ-p_{frag} relation in Figure 11b, while all the other parameters are held constant. These results show that decay of parent compounds is faster with increasing γ for both RH conditions.